Thermophysics and Aeromechanics, *2015*, *Vol. 22*, *No. 3*

Flow of polydisperse gas-particle mixture in a duct followed by coagulation in a nonlinear wave field*

A.L. Tukmakov[1], R.I. Bayanov[2], and D.A. Tukmakov[2]

[1]*Kazan National Research Technical University named after A.N. Tupolev*, *Kazan*, *Russia*

[2]*Institute of Mechanics and Mechanical Engineering of the Kazan Scientific Center of RAS*, *Kazan*, *Russia*

E-mail: tukmakov@mail.knc.ru

(*Received July 14*, *2014*; *in revised form January 23*, *2015*)

Numerical simulation of the flow of an aerosol of polydisperse composition in a plane duct, where the resonance acoustic oscillations are generated, which are directed across the flow, has been carried out. The peculiarities of the flow, which is followed by coagulation and alteration of the distribution of particles over their sizes, have been described. The carrying medium has been modeled with the aid of the system of Navier–Stokes equations for compressible heat-conducting gas. The polydisperse phase dynamics is described by the systems of equations involving the equations of continuity, conservation of the momentum and internal energy. Equations of the motion of carrying medium and disperse fractions are written with allowance for interphase exchange by the momentum and energy. A Lagrangian model has been used to describe the coagulation process. The dispersion alteration in the gas-particle flow under the action of acoustic oscillations, which are resonant for the duct cross section, is analyzed.

Key words: acoustic resonator, Navier–Stokes equations, motion equations for polydisperse gas-particle mixture, explicit MacCormack scheme, nonlinear and discontinuous oscillations, coagulation of particles.

Introduction

The quality of the separation of phases in separators of the inertial type depends on the dispersion of the vapor-gas-droplet flow. If there are in the flow the particles with the radius of the order of one micron and less, then one fails to separate them in inertial separators from the carrying medium by virtue of a small velocity delay with respect to the carrying phase. Such a phenomenon reduces the efficiency of the technologies for gasification of cryogenic liquids as well as the technologies for the water cleaning and desalination, which are based on the adiabatic atomization of liquids in nozzles [1] and on the centrifugal separators and vortex pipes, which are used for separation of phases. Numerous experimental works show that a vapor-gas-droplet medium of a polydisperse composition, which is non-equilibrium

* The work was financially supported by the Russian Ministry of Education and Science according to the Agreement about Grant No. 14.577.21.0151 on November 28, 2014.

© A.L. Tukmakov, R.I. Bayanov, and D.A. Tukmakov, 2015

in velocity, forms at the liquid atomization [2]. One can increase the efficiency of centrifugal separation at the expense of a preliminary acoustic action on the medium with the aid of nonlinear waves contributing to the coagulation of fine-dispersed fractions and a reduction of their concentration. In doing so, the choice of the wave effect intensity is limited by a critical Weber number [3] in order to ensure that the coagulation of particles at their collision predominates their fragmentation. To describe the dynamics of a coagulating polydisperse gas-particle mixture a mathematical model is applied, in which a certain fraction corresponds to each size of particles [4]. The carrying phase is described by the system of the Navier–Stokes equations with regard for the exchange of the momentum and energy with all disperse fractions. The disperse fraction includes n fractions, each of which is described by a system containing the continuity equation for the mean density, conservation equations for the momentum components, and the equation for the internal energy conservation, which are written with regard for the exchange of momentum and energy with the carrying medium. The process of particles coagulation is described with the aid of a Lagrangian model, which enables the consideration of an exchange of mass, momentum, and energy between fractions because of particles collisions [3, 5].

1. Equations of the motion of a multi-velocity multi-temperature polydisperse gas-particle mixture

As the carrying medium, the gas is considered. Its motion is governed by the system of the Navier–Stokes equations. The system of motion equations for the multi-velocity multi-temperature gas-particle mixture includes the system of motion equations for the carrying phase (1) and n systems of motion equations for disperse phases (2). The systems have the following form in Cartesian coordinates in the two-dimensional statement [4]:

$$\frac{\partial \rho}{\partial t}+\frac{\partial(\rho u)}{\partial x}+\frac{\partial(\rho v)}{\partial y}=0,$$

$$\frac{\partial(\rho u)}{\partial t}+\frac{\partial}{\partial x}\left(\rho u^2+p-\tau_{xx}\right)+\frac{\partial}{\partial y}\left(\rho uv-\tau_{xy}\right)=-\sum_{i=1,n}F_{xi}+\alpha\frac{\partial p}{\partial x}, \qquad (1)$$

$$\frac{\partial(\rho v)}{\partial t}+\frac{\partial}{\partial x}\left(\rho uv-\tau_{xy}\right)+\frac{\partial}{\partial y}\left(\rho v^2+p-\tau_{yy}\right)=-\sum_{i=1,n}F_{yi}+\alpha\frac{\partial p}{\partial y},$$

$$\frac{\partial(e)}{\partial t}+\frac{\partial}{\partial x}\left(\left[e+p-\tau_{xx}\right]u-\tau_{xy}v+\lambda\frac{\partial T}{\partial x}\right)+\frac{\partial}{\partial y}\left(\left[e+p-\tau_{yy}\right]v-\tau_{xy}u+\lambda\frac{\partial T}{\partial y}\right)=$$

$$=-\sum_{i=1,n}Q_i-\sum_{i=1,n}\left(\left|F_{xi}\right|(u-u_i)-\left|F_{yi}\right|(v-v_i)\right)+\alpha\left(\frac{\partial pu}{\partial x}+\frac{\partial pv}{\partial y}\right),$$

$$p=(\gamma-1)(e-\rho(u^2+v^2)/2),\quad e=I+\rho(u^2+v^2)/2\ ,\quad \alpha=\sum_{i=1,n}\alpha_i,$$

$$\tau_{xx}=\mu\left(2\frac{\partial u}{\partial x}-\frac{2}{3}D\right),\quad \tau_{yy}=\mu\left(2\frac{\partial u}{\partial y}-\frac{2}{3}D\right),\quad \tau_{xy}=\mu\left(\frac{\partial \mu}{\partial y}+\frac{\partial v}{\partial x}\right),\quad D=\frac{\partial u}{\partial x}+\frac{\partial v}{\partial y}.$$

Here ρ, u, v, u_i, v_i, e, λ, μ are the density, components of the velocities of the carrying and disperse phases, total energy, components of thermal conductivity and viscosity of the carrying phase, $\alpha=\sum_{i=1,n}\alpha_i$ is the volumetric content of the disperse phase, which is obtained by summation over the volumetric contents of fractions. The quantities F_{xi}, F_{yi}, and Q_i are determined by the laws of the interphase friction and heat exchange. $I = RT/(\gamma-1)$ is the gas internal

energy, R and γ are the gas constant and the air adiabatic constant. The dynamics of each component of disperse phase is described by the equation for the conservation of the mean density of disperse phase, conservation equations for the momentum components, and conservation equation for the internal energy [4]:

$$\frac{\partial \rho_i}{\partial t}+\frac{\partial(\rho_i u_i)}{\partial x}+\frac{\partial(\rho_i v_i)}{\partial y}=0,$$

$$\frac{\partial(\rho_i u_i)}{\partial t}+\frac{\partial}{\partial x}\left(\rho_i u_i^2\right)+\frac{\partial}{\partial y}(\rho_i u_i v_i)=F_{xi}-\alpha\frac{\partial p}{\partial x},$$

$$\frac{\partial(\rho_i v_i)}{\partial t}+\frac{\partial}{\partial x}(\rho_i u_i u_i)+\frac{\partial}{\partial y}\left(\rho v_i^2\right)=F_{yi}-\alpha\frac{\partial p}{\partial y}\ , \tag{2}$$

$$\frac{\partial(e_i)}{\partial t}+\frac{\partial}{\partial x}(e_i u_i)+\frac{\partial}{\partial y}(e_i v_i)=\mathrm{Nu}_i\frac{6\alpha_i}{(2r_i)^2}\lambda(T-T_i),$$

$$\rho_i=\alpha_i\rho_{i0},\ e_i=\rho_i C_{pi}T_i.$$

Here α_i, ρ_i, e_i, and T_i are the volume concentration, mean density, internal energy, and disperse phase temperature, C_{pi} and ρ_{i0} are the specific heat and density of the solid phase substance. The aerodynamic friction components F_x and F_y are determined as follows [4]:

$$F_{xi}=\frac{3}{4}\frac{\alpha_i}{(2r_i)}C_d\rho\sqrt{(u-u_i)^2+(v-v_i)^2}\,(u-u_i),$$

$$F_{yi}=\frac{3}{4}\frac{\alpha_i}{(2r_i)}C_d\rho\sqrt{(u-u_i)^2+(v-v_i)^2}\,(v-v_i),$$

$$C_{di}=C_{di}^0\psi(M_{i0})\varphi(\alpha_i),\quad C_{di}^0=\frac{24}{\mathrm{Re}_{i0}}+\frac{4}{\mathrm{Re}_{i0}^{0.5}}+0.4,\quad \psi(M_{i0})=1+\exp\left(-0.427/M_{i0}^{0.63}\right),$$

$$\varphi(\alpha_i)=(1-\alpha_i)^{-2.5},\quad \mathrm{Re}_{i0}=\rho\left|\bar{V}-\bar{V}_i\right|2r_i/\mu,\quad M_{i0}=\left|\bar{V}-\bar{V}_i\right|/c,$$

$$\mathrm{Nu}_i=2\exp(-M_{i0})+0.459\mathrm{Re}_{i0}^{0.55}\mathrm{Pr}^{0.33},\quad \mathrm{Pr}=\gamma C_p\mu/\lambda,\quad 0\le M_{i0}\le 2,\quad 0\le \mathrm{Re}_{i0}<2\cdot10^5.$$

The carrying medium temperature is found from the relation $T=(\gamma-1)(e/\rho-0.5(u^2+v^2))/R$. The internal energy of the solid phase suspended in gas is determined as $e_i=\rho_i C_{pi}T_i$. The coefficient of the gas thermal conductivity λ as well as the thermal flux due to the heat exchange between the gas and the particle: $Q_i=\alpha^{\mathrm{T}}4\pi r_i^2(T-T_i)n=6\alpha_i\cdot\mathrm{Nu}_i\cdot\lambda\cdot(T-T_i)/(2r_i)^2$ enter the energy equation for carrying phase, where $\mathrm{Nu}_i=2\cdot r_i\alpha^{\mathrm{T}}/\lambda$ is the Nusselt number, n is the concentration, r_i is the radius of particles.

The system of motion equations for the two-phase multi-temperature multi-velocity polydisperse medium was written in generalized moving coordinates and solved by the second-order explicit MacCormack method [6–8] with a scheme of nonlinear correction [9].

2. Model of the coagulation of aerosol particles

The equations for the evolution of mass, concentration, momentum, and temperature of disperse fractions because of coagulation may be written as follows [3]. The mass of the ith particle m_i (i = 2,…, n) increases at the expense of the absorption of finer jth

particles with the mass m_j (j = 1, 2, …i – 1): $\frac{dm_i}{d\tau} = \sum_{j=1}^{i-1} k_{ij} n_j m_j$, where $k_{ij} = k_{ij}^0 \pi (r_i + r_j)^2 \times$ $\times \left[u_j \cos(\beta) + v_j \sin(\beta) - \sqrt{u_i^2 + v_i^2} \right]$ is the coagulation constant, $\beta = \text{arctg}(v_i/u_i)$, r_i is the radius of particles of the i-fraction, $r_i > r_j$. Under the assumption on the coagulation of particles, the correction coefficient $k_{ij}^0 = 1$ in all cases of the contact. The coefficient k_{ij}^0 can generally be determined as the number of the collisions with coagulation per the total number of collisions for the particles of the ith and jth fractions. A new value of the mass of the particles of the ith fraction in the current node of the finite-difference grid enables one to determine a new value of the particle radius r_i. A reduction of the concentration of the jth particles due to their absorption by the larger ith ones ($i = j + 1, j + 2, \ldots n$) is described by the equation $dn_j/d\tau = -n_j \sum_{i=j+1}^{n} k_{ij} n_i$, ($j$ = 1, 2,…, n – 1). A new value of the volumetric content of the ith fraction, which has changed due to coagulation, is determined as $\alpha_i = 4/3\pi r_i^3 n_i$. The concentration n_i is determined in terms of the mean density and the radius of the ith fraction at each step of computations. The confluence of fine droplets with the larger ones leads to a change of their velocity: $dw_i/d\tau = \frac{1}{m_i} \sum_{j=1}^{i-1} k_{ij} \left(w_j - w_i \right) m_j n_j$. The temperature of the particle of the ith fraction after the coagulation with the particles of finer fractions was found from the relation: $T = \frac{1}{Cm} \left(\sum_{j=1}^{i-1} k_{ij} n_j C_j m_j T_j + C_i m_i T_i \right)$, where T, C, and m are the temperature, specific mass heat capacity, and the mass of the particle of the ith fraction after the coagulation, T_i, C_i, and m_i are the same parameters prior to coagulation. The changes in velocity and temperature of the disperse phase, which are caused by coagulation, were taken into account at each time step of the main algorithm.

3. Results of the computations of flow and gas-particle mixture coagulation in a plane duct under the acoustic field action

Let the gas-particle mixture consisting of five fractions with the particle radii r_{10} = 1 μm, r_{20} = 5 μm, r_{30} = 10 μm, r_{40} = 15 μm, r_{50} = 20 μm and being in a suspended state move at the initial moment of time at the velocity u_0 = 35 m/s and fills uniformly a plane duct (Fig. 1). The duct length L = 0.5 m, the height d = 0.06 m. The density of the particles substance ρ_{10} = = ρ_{20} = ρ_{30} = ρ_{40} = ρ_{50} = 1000 kg/m^3. The initial mean density of disperse fractions ρ_1 = ρ_2 = ρ_3 = = ρ_4 = ρ_5 = 0.000025 kg/m^3, the air density ρ_0 = 1.21 kg/m^3. The temperature of the carrying and disperse phase at the initial moment of time T = 343 K. The specific heat of the disperse fraction substance C = 4.2 kJ/kg·K. The slip conditions are set on duct walls for the velocity of the carrying and disperse fractions; for all remaining gas-dynamic functions, including the inlet and outlet boundaries, the homogeneous boundary conditions of the second kind are set. At $t > 0$, the process of in-phase oscillations of the transverse velocity component of the intervals of the upper and lower duct walls starts

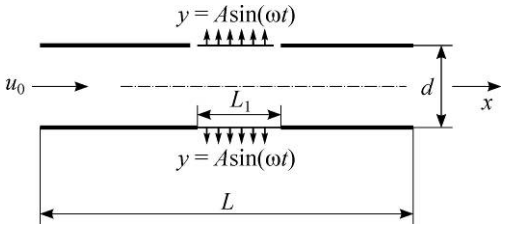

Fig. 1. Channel scheme with a resonant site.

$((L - L_1)/2 < x < (L + L_1)/2, y = 0)$, $((L - L_1)/2 < x < (L + L_1)/2, y = d)$ according to the law $v(t) = A \cdot \sin(\omega t)$ (Fig. 1), which leads to the generation of oscillations in the carrying and disperse phases. The oscillator length $L_1 = 0.1L$. The oscillation frequency is equal to the first eigenfrequency with respect to the duct cross section $\omega = \pi c/d$, where $c = (\gamma RT)^{1/2}$ is the sound velocity in gas at a given temperature. The computations were done on an orthogonal grid containing 200×30 nodes in the longitudinal and transverse directions.

4. Flow and coagulation of the gas-particle mixture at the first eigenfrequency of resonance oscillations of the gaseous column in the transverse direction

Figures 2*a* and 2*b* show the temporal dependencies of the longitudinal and transverse components of the velocity of the carrying and disperse phase of five fractions in the flow on which a standing wave field with the first eigenfrequency of transverse oscillations of the gaseous column and the amplitude A = 0.0003 m of the oscillations of the transverse velocity component on the walls acts locally. The oscillations of the transverse velocity component are nonlinear, with a steep leading front and a gentle rear front. The amplitude of oscillations of the transverse velocity component reaches 60 m/s (Fig. 2*a*). The velocity slip of the carrying phase and the finest fraction (r_1 = 1 μm) is insignificant, the velocity curves are very close (Fig. 2*b*). With the increasing radius of particles, the amplitude of the velocity oscillations of the solid fraction decreases, the temporal delay of the variation of the disperse phase velocity relative to the carrying medium increases. The highest value of the Weber number for the fraction of water droplets with radius r = 20 μm is reached in the loop of standing waves and makes $\mathrm{We}_{\max} = 2\rho r_{50} \max|u - u_5|/\sigma = 4.4$, where ρ and σ are the carrying medium density and the surface tension coefficient of water. Thus, $\mathrm{We}_{\max}$ is less than the critical range of the Weber numbers $\mathrm{We}_{\mathrm{cr}}$ = 10–20. Hence, one can suppose that the particles retain their stability at collisions, and their coagulation is a predominant process at the collisions of droplets. During one period of the oscillations of the transverse velocity component, there occur two periods of the longitudinal component oscillations (Figs. 2*a* and 2*b*). At the initial moment of time the velocities of the carrying phase and disperse fractions are equal. The motion velocity of solid fractions in the longitudinal direction decreases with time. Velocity oscillations in the axial direction lag in phase from the oscillations of the transverse velocity component, and the maxima of the transverse acceleration component correspond to the maxima of the longitudinal velocity component. The minima of the longitudinal velocity component correspond to the maxima of the transverse velocity component (Figs. 2*a* and 2*b*).

Figures 3*a* and 3*b* show the functions describing the changes of the gas-particle mixture dispersion with time due to coagulation. The radii of particles of all fractions, except for

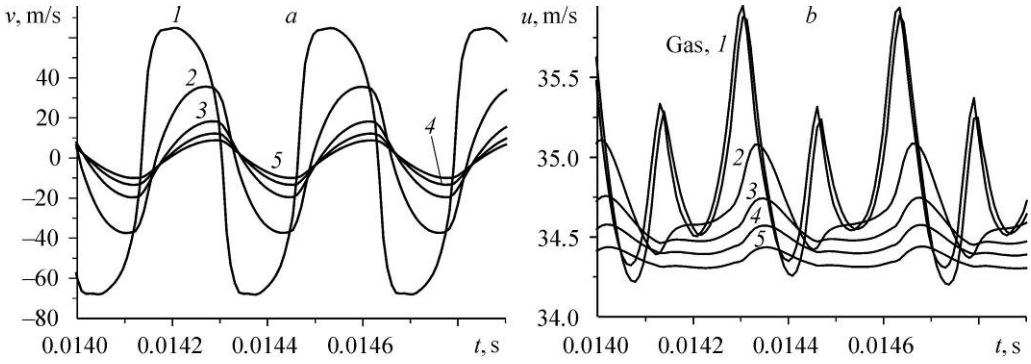

Fig. 2. Temporal dependences of speeds of fractions at point (*L*/2, *d*/2).
Velocity components: the transverse component (*a*), axial component (*b*);
R_0 = 1 μm (*1*), 5 μm (*2*), 10 μm (*3*), 15 μm (*4*), 20 μm (*5*).

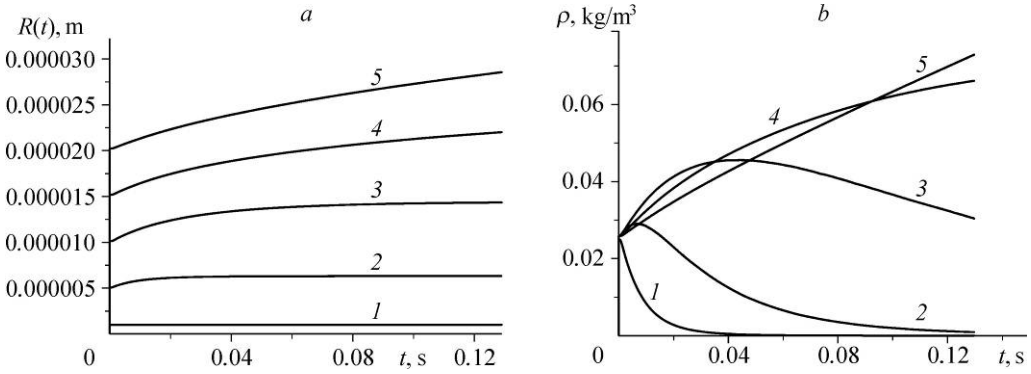

Fig. 3. Temporal dependencies at point ($x = L/2$, $y = d/2$).

a — the radius of aerosol particles with the initial radius R_0 = 1 μm (*1*), 5 μm (*2*), 10 μm (*3*), 15 μm (*4*), 20 μm (*5*); *b* — mean density of disperse fractions with the initial radius of particles R_0 = 1 μm (*1*), 5 μm (*2*), 10 μm (*3*), 15 μm (*4*), 20 μm (*5*).

the finest one, grow with time (Fig. 3*a*), whereas the mean density of fractions changes nonmonotonously. The fraction mean density with particles radius 1 μm monotonously drops in time and nearly vanishes by the moment of time t = 0.04 s. The mean density of larger fractions (5 μm, 10 μm, and 15 μm) at first reaches the highest value, and after that, decreases monotonously. At the same time, the mean density of the largest fraction permanently increases with time (Fig. 3*b*).

Figures 4*a* and 4*b* show the functions characterizing the variation of the dispersion of solid fractions by the moment of time t = 0.15625 s. The highest rate of the diminution of the concentration

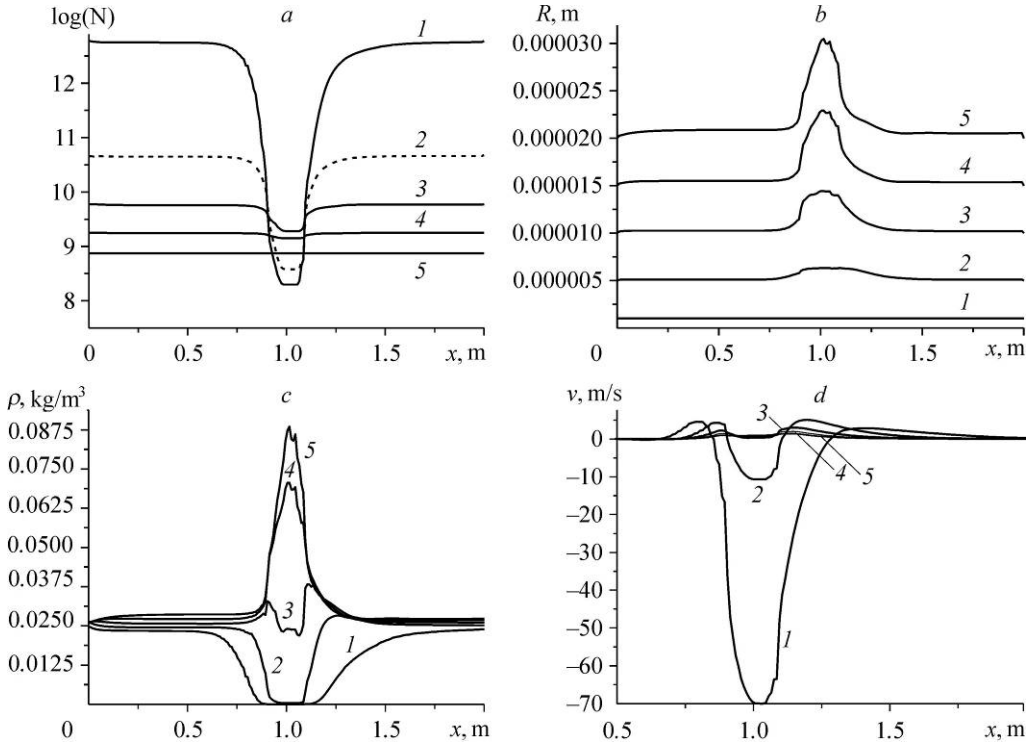

Fig. 4. Characteristics of dispersion of solid fractions and the transverse velocity component of fractions along the channel axis ($y = d/2$) at the moment of time t = 0.15625 s.

a — distribution of concentrations, *b* — radii of particles of fractions, *c* — mean density of fractions, *d* — transverse velocity component of fractions; R_0 = 1 μm (*1*), 5 μm (*2*), 10 μm (*3*), 15 μm (*4*), 20 μm (*5*).

of particles because of their coagulation in the acoustic field is observed for the finest fraction. In the neighborhood of the source of acoustic oscillations, the concentration of particles with the radius of 1 μm drops by about four orders of magnitude (Fig. 4*a*). The effective radius of particles of all fractions, except for the finest one, rapidly increases in the same region (Fig. 4*b*). A zone extended downstream forms, in which the mean density of fine dispersed fractions drops, and the mean density of the fraction of particles with R_0 = 20 μm increases (Fig. 4*c*). Thus, the action of resonance wave fields on the coagulating gas-particle mixture flow enables one to reduce efficiently the concentration of fine dispersed fractions, which may be used as a preliminary stage for increasing the efficiency of separating the phases in the separators of inertial type.

References

1. **Patent** No. 2347934 RF, MPK[51] F02M21/02, V.G. Tonkonog and S.N. Arslanova, System for Supplying Cryogenic Fuel to Power Setup. Declarant and patent owner the A.N. Tupolev Kazan State Techn. University, No. 2007129998/06; declared 06.08.2007; published 27.02.2009.
2. **Yu.A. Lozhkin, D.M. Markovich, M.A. Pakhomov, and V.I. Terekhov,** Investigation of the structure of a polydisperse gas-droplet jet in the initial region. Experiment and numerical simulation, Thermophysics and Aeromechanics, 2014, Vol. 21, No. 3, P. 293–307.
3. **V.E. Alemasov, A.F. Dregalin, A.P. Tishin, and V.A. Khudyakov,** Thermodynamic and Thermophysical Properties of Combustion Products: Handbook in 5 Volumes. Vol. 1. Computational Techniques, VINITI, Moscow, 1971.
4. **A.G. Kutushev,** Mathematical Modelling of Wave Processes in Aerodisperse and Powder-like Media, Nedra, St. Petersburg, 2003.
5. **A.A. Shreiber,** Multiphase Polydisperse Flows with Variable Fraction Composition of Disperse Inclusions, in: Itogi nauki i tekhniki. Seriya: Kompleksnye i spetsialnye razdely mekhaniki. T. 3. VINITI, Moscow, 1988, P. 3–80.
6. **A.L. Tukmakov,** Numerical simulation of oscillations of a monodisperse gas-particle mixture in a nonlinear wave field, J. Appl. Mech. Tech. Phys., 2011, Vol. 52, No. 2, P. 186–192.
7. **C.A.J. Fletcher**, Computational Techniques for Fluid Dynamics. Vol. 2, Springer-Verlag, Berlin, 1988.
8. **J.L. Steger,** Implicit finite-difference simulation of flow about arbitrary two-dimensional geometries, AIAA J., 1978, Vol. 16, No. 7, P. 679–686.
9. **A.I. Zhmakin and A.A. Fursenko,** On a monotonic shock-capturing difference scheme, USSR Comp. Math. Math. Phys., 1980, Vol. 20, No. 4, P. 218–227.